NUCLEATION MODELLING ON ZNO ELECTRODEPOSITION

J. Orozco-Messana[1], M. Mahon[2], <u>M.Iborra</u>[1]

[1]Universitat Politecnica de Valencia, Ed. Nexus 4ªplanta, Camino Vera s/n, 46022 Valencia (Spain)
jaormes@upv.es
[2]University of British Columbia, 2366 Main Mall, Vancouver V6T 1Z4 (Canada)

Resumen: Short ZnO nanorods have been produced on ITO covered glass substrates by pulsed electrodeposition. The role of reactants and droplet interfaces on the nucleation and growth of ZnO nanorods have been investigated. A conceptual model for nucleation of ZnO nanorods has been proposed by describing the half-oxidation and reduction reactions at the growth front. The importance of limit layer [OH-] on the nucleation phenomena has been studied by assesing difussion through the finite differences electrochemical model. Atomic force microscopy (AFM), scanning electron microscopy (SEM), transmission electron microscopy (TEM) and electrochemical quartz crystal microbalance (EQCM) analysis have been used to characterize ZnO nanorods and investigate the nucleation model.

Palabras clave: ZnO, nanorods, electrodeposition speciation model.

1. INTRODUCTION.

The use of zinc oxide as a semiconductor has many applications such as in dye-sensitized solar cells [1]. Using zinc oxide for solar cell applications is attractive because it is an inexpensive material with a wide band gap (3.37 eV) and high electron mobility [6]. Zinc oxide applied as a thin film has been shown to produce viable solar cells. These thin films can be through high temperature processes with vapour phase or vacuum methods, hydrothermally through the precipitation as well as electrodeposition in aqueous systems [2]. Electrodeposition is an attractive method of processing these thin films for industrial purposes because it can be applied to a large conductive area with a low (<100 Co) temperature requirement in an aqueous system. The band gap can be further manipulated through the resulting morphology of the crystal structure or the addition of impurities based on the desired characteristics. However controlling these two parameters can be difficult. The morphology is known to vary with the temperature, concentration, mixing and current applied to the system and the system is not fully understood.

Development of a model to better understand this system is proposed in order to better understand the system and identify ideal parameters and methodologies for the large scale electrodeposition of zinc oxide.

2. MODEL DEVELOPMENT.

To understand better the conditions of the model, first a mechanism of deposition is needed. Previous models have been suggested dealing with the electrodeposition of zinc oxide [2], however this model does not take in to account the speciation of zinc through the variance in pH, and or kinetic constants. The model will be based on an aqueous system at a near neutral starting pH of 6, with bubbling providing oxygen and mixing to the system. Electrodeposition of zinc oxide is recognized to occur in two steps, first reduction to produce hydroxide. Hydroxide then reacts with zinc ions to deposit zinc oxide.

$$O_2 + 2H_2O + 4e^- \rightarrow 4OH^-$$
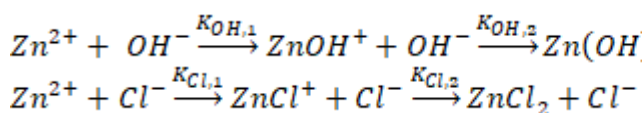$$Zn^{2+} + 2OH^- \rightarrow ZnO + H_2O$$
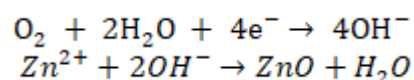
Zinc oxide crystals typically exhibit an HCP wurtzite crystal structure. These crystals can grow to form platelets, columns, hollow columns, and flower like arrangements [6]. The growth of each of these types of arrangements is thought to be a product of the nucleation rate and the preferred growth direction of the crystal. For a hexagonal crystal, the growth will occur primarily in two directions, along the c-axis or along the [0001] direction which will result in long, thin, high aspect ratio crystals giving hexagonal columnar growth, or growth occurs on the family of planes, resulting in wide flat crystals. The nucleation rate will determine the density of crystals formed, which can occur either progressively where new nuclei are formed throughout the deposition time, or instantaneously where nuclei are formed only in the initial moments of deposition [3]. For applications in solar cells, a uniform deposition of compact vertically aligned columns is desired.

Models of zinc oxide deposition have been proposed in Ref. [4]. The model [3] focused on the nucleation rate of the reaction, noting that zinc oxide will typically occur instantaneously. However, there is a progressive nucleation of Zn(OH)2 on the surface as well. Zinc hydroxide has been observed to form a thin base layer on at the substrate surface. Progressive nucleation is indicative of a formation and redissolution of the zinc hydroxide layer. Mackay et al. demonstrated the application of a two dimensional finite element analysis (FEA) to analyze the availability of Zn^{2+} and OH- to nucleated crystals. However two problems with this model exist. First is the difficulty of predicting species

concentration in the small element volumes, and second the chemical species are limited to free Zn^{2+} and free OH^-. This second concern is important because the speciation of zinc, chloride and hydroxide must be taken in to account because the availability of certain species to the surface will have an effect on the growth kinetics.

Speciation leads to the creation of two speciation chains. We assume these happen instantaneously within the aqueous system given the low concentrations and the relatively slower rate of solid deposition.

$$Zn^{2+} + OH^- \xrightarrow{K_{OH,1}} ZnOH^+ + OH^- \xrightarrow{K_{OH,2}} Zn(OH)_2 + OH^- \xrightarrow{K_{OH,3}} Zn(OH)_3^- + OH^- \xrightarrow{K_{OH,4}} Zn(OH)_4^{2-}$$

$$Zn^{2+} + Cl^- \xrightarrow{K_{Cl,1}} ZnCl^+ + Cl^- \xrightarrow{K_{Cl,2}} ZnCl_2 + Cl^- \xrightarrow{K_{Cl,3}} ZnCl_3^-$$

Equilibrium constants (K) for each reaction can be predicted based on the assumption that net free energy of formation at the temperature of the system is zero. Using these equilibrium constants we can predict the concentration of each species available in the solution based on the total amount of species available using the following equation.

$$[M]_T = [M] + \sum_{i=1}^{n}\sum_{j=1}^{m} \beta [M][L(j)]^i \frac{\gamma_M \gamma_{L(j)}^i}{\gamma_{M(L(j))_n}}$$

where $[M]_T$ is the total amount of metal ion, $[M]$ is the available (or free) concentration of the metal, L(j) is the available concentration of the ligand (OH^- or Cl^-), is the activity coefficient of each species, i is the number of speciation steps to a maximum of n (e.g. i = 1 for $ZnOH^+$, i = 2 for $Zn(OH)_2$ etc.), j is the ligand to the total number of different ligands m (m = 2 in this case) and is the overall formation constant of the species.

Similar expressions can be written for $[L(j)]_T$ as well. This is important since the total concentration of chloride, zinc and hydroxide ions are known. Notably, the total hydroxide concentration will increase, the total zinc concentration will decrease and the total chloride will stay constant.

Prediction of the activity coefficients can be done with Debye-Hückel equation

$$\log(\gamma_z) = -0.51 z^2 \left(\frac{\sqrt{I}}{1+\sqrt{I}} - 0.3I \right)$$

where z is the ionic charge and I is the ionic strength of the solution given by:

$$I = \frac{1}{2}\sum_{1}^{n} c_i z_i^2$$

It must be noted that the Debye-Hückel equation is suitable for low concentrations of species as it relies on an estimation of the radius of ionic interaction. Other models such as the Davies or Pitzer model which are extensions of the Debye-Hückel equation can offer more comprehensive predictions of activity coefficients

at the cost of magnified mathematical complexity. For this work, given the low concentrations of species and static temperature of the model, the Debye-Hückel equation was deemed reasonable.

Each speciation reaction has an equilibrium constant K.

$$M(L(j))_n^{z+} + L(j)^+ \xrightarrow{K_i} M\left((L(j))^{(1+z)+}\right)_{n+1}$$
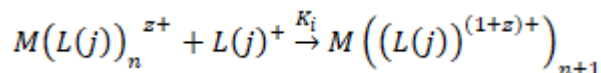
The overall reaction from the most basic components has an overall formation constant β, with the overall formation constant being the product of all of the equilibrium constants before it.

$$M^{z+} + nL(j)^+ \xrightarrow{\beta_i} M(L(j))_n^{(n+z)+}$$
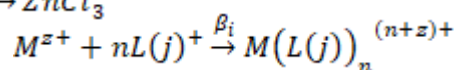
With:

$$\log\beta_i = \sum_{1}^{n} \log K_i$$

Using Gibbs free energy of formation we can generate temperature dependent relations of the equilibrium constants and the inverse of temperature as presented in Table 1. The values generated by these relations correspond with experimental K values reported at 25°C [5].

Table 1. Equilibrium and Formation constants for the speciation of Zn^{2+} with OH^- and Cl^- at varying temperature (K)

speciation equation	$log(K)$	overall equation	$log(\beta)$
Zn^{2+} + OH^- →$ZnOH^+$	$-1199\left(\frac{1}{T}\right) + 10.2$	Zn^{2+} + OH^- →$ZnOH^+$	$-1199\left(\frac{1}{T}\right) + 10.2$
$ZnOH^+$ + OH^- →$Zn(OH)_2$	$2354\left(\frac{1}{T}\right) + 2.04$	Zn^{2+} + $2OH^-$ →$Zn(OH)_2$	$1155\left(\frac{1}{T}\right) + 12.2$
$Zn(OH)_2$ + OH^- →$Zn(OH)_3^-$	$307.7\left(\frac{1}{T}\right) + 2.85$	Zn^{2+} + $3OH^-$ →$Zn(OH)_3^-$	$1462\left(\frac{1}{T}\right) + 15.1$
$Zn(OH)_3^-$ + OH^- →$Zn(OH)_4^{2-}$	$613.3\left(\frac{1}{T}\right) + 0.883$	Zn^{2+} + $4OH^-$ →$Zn(OH)_4^{2-}$	$2076\left(\frac{1}{T}\right) + 15.9$
Zn^{2+} + Cl^- → $ZnCl^+$	$-2484\left(\frac{1}{T}\right) + 8.56$	Zn^{2+} + Cl^- → $ZnCl^+$	$-2484\left(\frac{1}{T}\right) + 8.56$
$ZnCl^+$ + Cl^- → $ZnCl_2$	$-1585\left(\frac{1}{T}\right) - 1.78$	Zn^{2+} + $2Cl^-$ → $ZnCl_2$	$-4069\left(\frac{1}{T}\right) + 6.78$
$ZnCl_2$ + Cl^- → $ZnCl_3^-$	$2357\left(\frac{1}{T}\right) - 2.63$	Zn^{2+} + $3Cl^-$ → $ZnCl_3^-$	$-1712\left(\frac{1}{T}\right) + 4.15$

3. REACTION KINETICS.

The reaction kinetics must reflect the production of the various species through the time. As noted in Ref. [3] there is a progressive nucleation of $Zn(OH)_2$ and a

instantaneous nucleation of ZnO. The $Zn(OH)_2$ forms a thin amorphous layer on the substrate in initial times of deposition, while continuing further in time, ZnO deposition dominates growth. This gives us the basic rate for the precipitation reactions.

$$k_o = A_o \exp\left(\frac{-E_a}{RT}\right)$$
$$r_i = n_i k_o \prod_i a_i^{n_i}$$

where A_o is the frequency factor of the reaction (s-1), E_a is the driving force of the reaction (J/mol),   is the gas constant (J/mol•K), T is the temperature (K), a_i is the rate constant,   is the activity of reacting species i, n_i , i is the number of mols species   reacting, and r is the reaction rate (mol/s).

Table. 2 Reaction kinetics

Reaction Equation	k_o	Rate Form
$Zn^{2+} + 2OH^- \rightarrow ZnO + H_2O$	k_1	$k_1 a_{Zn^{2+}} a_{OH^-}^2$
$ZnOH^+ + OH^- \rightarrow ZnO + H_2O$	k_2	$k_2 a_{ZnOH^+} a_{OH^-}$
$Zn^{2+} + 2OH^- \rightarrow Zn(OH)_2$	k_3	$k_3 a_{Zn^{2+}} a_{OH^-}^2$
$ZnOH^+ + OH^- \rightarrow Zn(OH)_2$	k_4	$k_4 a_{ZnOH^+} a_{OH^-}$
$Zn(OH)_{2,(aq)} \rightarrow ZnO + H_2O$	k_5	$k_5 a_{Zn(OH)_{2,(aq)}}$

The values of constants are fitted to the EQCM curves obtained. From Fig.1 we can distinguish three primary regions. An initial period of Zn(OH)2 deposition which transitions in to the second linear portion of particular interest which indicates a deposition of ZnO. In the final region the value of RE decreases which is indicative of some barrier to deposition given that the current is still being applied.
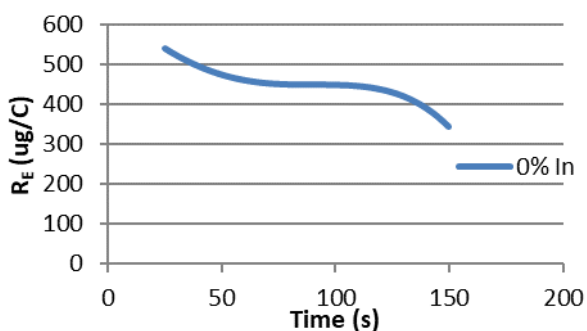

Fig.1 EQCM kinetic regions.

The same slope data can be generated for every time step in the ANSYS simulation. Using this a procedure to determine the constants is implemented as shown in Fig. 2.
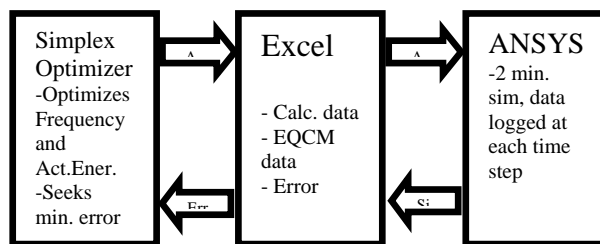

Fig.2 Mathematical procedure for model determination.

To solve for these activation energy and frequency factor, we require EQCM data for multiple temperatures, otherwise the optimized variable pairs are over determined, and will balance each other at arbitrary values. However we only have data for 69ºC. To overcome this, for now we set all activation energies to 0, thereby setting the exponential to 1, leaving the frequency factor to vary. This effectively solves for k_o instead of the frequency factor. Further temperature trials are needed to obtain both of these constants. The rates must account for total amounts of species, this gives the following three primary rate equations. This generates and consumes the critical three species (Zn, OH, O_2) at the cathode interface.

We can solve for the linear portion of the of the curve first where we know that we have growth of ZnO. This requires solving for k_1 and k_2 using an optimization of the simulation. A high mesh resolution at the cathode surface is used within CFX giving a calculation time of approximately 5 minutes per iteration to solve for ten points. Fluid movement is assumed to be turbulent with a velocity of 0.001 m/s of solution moving across the surface. This turbulent flow ensured a steady supply of zinc ions and dissolved oxygen to the surface. Turbulent flow is assumed to be created by the buoyant nature of the oxygen bubbles passing by the cathode. Limits were chosen to give a minimum of no contribution to mass deposition (0) and a maximum that gives a deposition mass an order larger than the experimental values. This resulted in $0 < k_1 < 10^{13}$ and $0 < k_2 < 10^6$. The values of these parameters will be a function of the appropriate availability of each species. Using this method a good fit is obtained for the linear portion representing ZnO deposition where $k_1 = 6.8 \times 10^{10}$ and $k_2 = 2.9 \times 10^5$.

Fig.3 shows a good match of the model to be used in further work for the optimization of the electrodeposition cycles design.
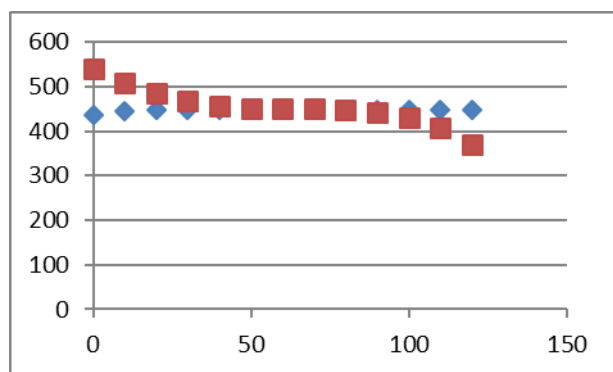
4. Acknowledgements

Fig.3 Model (◆) vs. experimental (■) results.

5. References

[1] Pradhan B, Batabyal S K, Pal A J. Vertically aligned ZnO nanowire arrays in Rose Bengal-based dye-sensitized solar cells[J]. Solar Energy Materials & Solar Cells 2007, 91,769–773.

[2] Lincot D. Electrodeposition of semiconductors Thin Solid Films 2005, 487(1), 40-48.

[3] Reyes-Tolosa M D, Orozco-Messana J, Damonte L C, et al. ZnO nanoestructured layers processing with morphology control by pulsed electrodeposition. J. Electrochem. Soc. 2011, 158(7), 452-455.

[4] Mackay J R, White S P, Hendy S C. Modelling the growth of zinc oxide nanostructures. ANZIAM Journal 2009: 50(3), 395-406.

[5] Zirino A, Yamamoto S. A pH-dependent model for the chemical speciation of copper, zinc, cadmium, and lead in seawater. Limnology and Oceanography, September 1972, 17(5), 661-671.

[6] Xu, F.; Dai, M.; Lu, Y.; Sun, L.; Hierarchical ZnO nanowire-nanosheet architectures for high power conversion efficiency in dye-sensitized solar cells. J. Phys. Chem. C 2010, 114, 2776–2782.